

## TOWARDS STABLE 18% EFG HIGH EFFICIENCY SOLAR CELLS – IMPROVED CELL PROCESS USING BULK HYDROGENATION VIA PECVD SiN

M. Kaes<sup>1</sup>, G. Hahn<sup>1</sup>, Th. Pernau<sup>1,3</sup>, A. Metz<sup>2</sup>

<sup>1</sup> University of Konstanz, Department of Physics, P.O.Box X916, 78457 Konstanz, Germany

<sup>2</sup> RWE SCHOTT Solar GmbH, Carl-Zeiss-Str. 4, 63755 Alzenau, Germany

<sup>3</sup> now at Centrotherm GmbH + Co. KG, Johannes-Schmid-Str. 3, 89143 Blaubeuren, Germany

Author for correspondence: Martin.Kaes@uni-konstanz.de, Tel.: +497531882082, Fax: +497531883895

**ABSTRACT:** With the help of a reliable photolithography based solar cell process and lifetime studies by  $\mu$ -PCD measurements we investigated state of the art EFG material. It was found that hydrogenation by firing a hydrogen rich silicon nitride layer boosts the typical low as grown lifetimes to remarkable values and that this method of hydrogenation is favorable compared to hydrogenation via a microwave induced remote H-plasma. However, it was discovered that after hydrogenation by a SiN firing step in a conventional belt furnace a subsequent hydrogenation by a H-plasma leads to further improved lifetimes and IV data. The bulk resistivity of the EFG wafers has a strong effect on the efficiency of the solar cells and its influence has been analyzed in the range of 1–6  $\Omega$ cm.

**Keywords:** Ribbon Silicon, Passivation, Doping

### 1 INTRODUCTION

To investigate the efficiency potential of solar cells processed from cost effective EFG Si wafers, the development of a stable cell process is needed. The main issue hereby is to increase the typical low as grown lifetimes during cell processing to a high level that hardly limits the cell efficiencies of e.g. an industrial type solar cell process. In several publications the important role of gettering and subsequent hydrogenation to increase EFG quality [1, 2, 3] was discussed. It turned out that a hydrogenation step by firing a hydrogen rich silicon nitride layer is essential to increase low as grown lifetimes in the range of microseconds by a factor of 10–100. Rohatgi et. al [1] demonstrate impressively the effectiveness of the hydrogenation by using a rapid thermal anneal of a SiN layer leading to record efficiencies of 18.2% for EFG. Unfortunately a fast degradation could be observed on solar cells processed according to this scheme [4]. In contrast to the RTP approach we focus on hydrogenation either by firing a SiN layer in a conventional belt furnace and/or hydrogenation by a microwave induced remote hydrogen plasma (MIRHP), both leading to not degrading solar cells on EFG material [3,5]. Hereby it turned out that hydrogenation by firing a SiN layer leads to significant higher bulk lifetimes than for hydrogenation by MIRHP [3].

Earlier studies showed that for EFG the bulk resistance should be above 3  $\Omega$ cm [6]. Higher dopant concentrations lead to a strong decrease of material quality. As the material quality of EFG was improved over the last years the authors investigated on solar cell level which dopant concentration seems to be optimal for current EFG wafer production.

### 2 LIFETIME TESTS

#### 2.1 Experimental Set-up

All lifetime measurements were carried out under low level injection conditions with a commercial  $\mu$ -PCD (microwave photo conductance decay) equipment (Janus 300 from Amecon). Structures like emitter, Al-BSF and SiN have been etched off before the measurements and

the wafer surfaces were passivated with an iodine ethanol solution during the measurement for a reliable measurement of the bulk lifetimes [2]. Adjacent EFG wafers were measured before and after gettering followed by hydrogenation and results of this experiment were discussed in detail in [3].

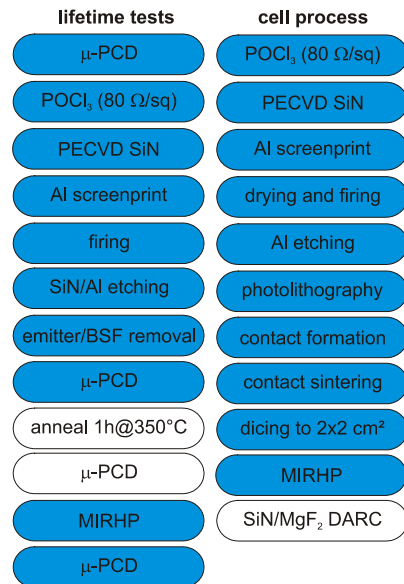


**Figure 1:** Processing sequence for the lifetime tests (left) to analyze the effect of hydrogenation by firing a SiN layer followed by MIRHP and solar cell process applied (right).

Two 5x5 cm<sup>2</sup> EFG wafers (3  $\Omega$ cm) underwent a second hydrogenation step by MIRHP to check if the lifetimes can be further improved (figure 1, left). Results of this second hydrogenation are discussed in the following section.

## 2.2 Lifetime results

The additional hydrogenation using MIRHP has a strong effect on the already well passivated EFG wafer after SiN firing. Poor wafer quality areas with as grown lifetimes below 0.5  $\mu$ s could be increased after gettering and hydrogenation by firing the SiN to about 50  $\mu$ s and furthermore to about 200  $\mu$ s after additional hydrogenation by MIRHP (area B). However, some areas could not be successfully passivated leading to lifetime values below 10  $\mu$ s after hydrogenation (area A).

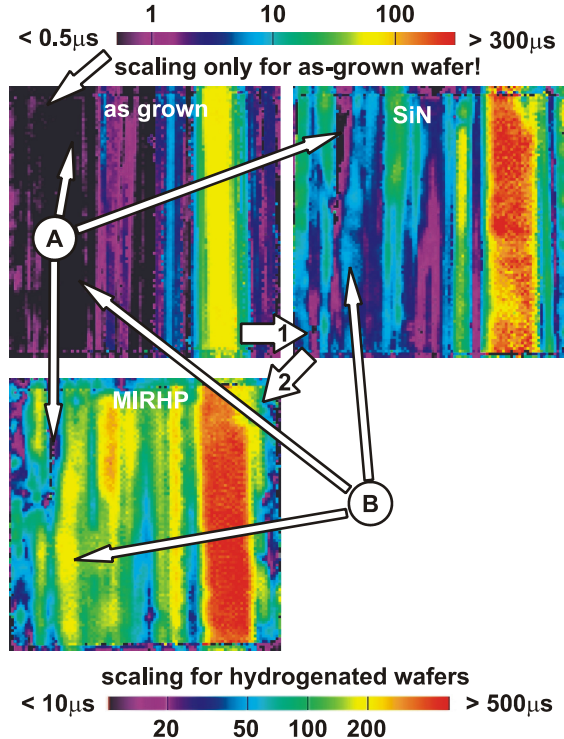


**Figure 2:**  $\mu$ -PCD lifetime mappings of a  $5 \times 5 \text{ cm}^2$  EFG wafer in the as grown state (upper left), after phosphorous gettering and hydrogenation by firing a SiN layer (upper right), and after additional hydrogenation by MIRHP (2 h@350°C, lower left). Note the different scalings.

To make sure that the second lifetime improvement is really due to a hydrogen passivation, a second wafer was annealed in H<sub>2</sub> ambient at 350°C for 1 h without plasma ignition (figure 3, lower right). Thus no significant indiffusion of hydrogen into the EFG wafer is expected. Except for some artefacts no differences in bulk lifetimes are observed. Thus the thermal treatment alone can not explain the lifetime improvement observed in figure 2 for the MIRHP hydrogenation. Again, after igniting the H-plasma (figure 3, lower left) the lifetimes are significantly improved comparable to the results in figure 2. Therefore it is proven that the observed lifetime improvements by the second hydrogenation using MIRHP are an effect of additional indiffusion of hydrogen from the H-plasma.

The reached bulk lifetimes with a mean value above 100  $\mu$ s should be high enough to process solar cells on EFG material comparable in efficiency to cells from standard ingot cast multicrystalline Si wafers.

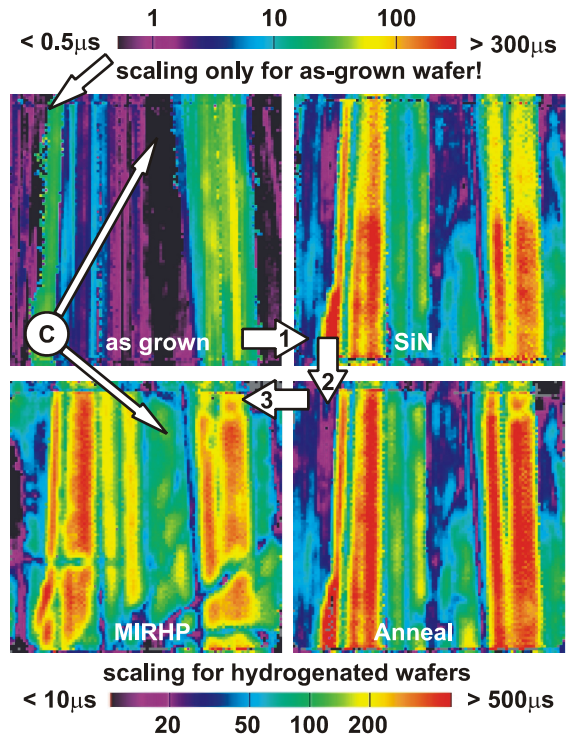


**Figure 3:**  $\mu$ -PCD lifetime mappings of a  $5 \times 5 \text{ cm}^2$  EFG wafer before hydrogenation (upper left), after gettering and hydrogenation by firing a SiN layer (upper right), after a thermal anneal with H<sub>2</sub> ambient (1 h@350°C, lower right) and after additional hydrogenation by MIRHP (1 h@350°C, lower left).

## 3 SOLAR CELL PROCESSING

### 3.1 Processing scheme

The EFG solar cells presented in this contribution are processed according to the sequence shown in figure 1 (right). IV data given are for untextured solar cells with a DARC using a 63.5 nm thick SiN layer ( $n_{\text{SiN}}=2.13$ ) as the first layer and a 100 nm thick MgF<sub>2</sub> layer ( $n_{\text{MgF}_2}=1.38$ ) as the second layer of the DARC (if mentioned some values are without this second layer).

### 3.1 Limitation of the applied process

The PC1D [7] simulation (figure 4) accurately fits the obtained efficiency values for monocrystalline FZ (Table I) and reveals the efficiency limit of the currently applied process. Solar cells according to this process reaching 18% efficiency are mainly limited by the rear side recombination velocity of the aluminum back surface field and are barely limited by the minority carrier lifetime. The processed EFG solar cells are mainly limited by bulk lifetimes, more precisely by the distribution of the lowest lifetimes in the poor wafer areas. The process could be improved in several ways to improve the IV data partly independent of minority carrier lifetimes: by reducing the grid shadowing (which is currently oversized with 4-4.5%) and by defining the solar cells on a larger silicon substrate. The currently applied dicing of the  $2 \times 2 \text{ cm}^2$  solar cells out of a larger substrate leads to a high  $j_{02}$  because of the unfavorable ratio of edge length to cell area.

### 3.2 Effect of EFG bulk resistivity on efficiency

As the simulation in figure 4 illustrates, the base resistivity has a strong influence on the efficiencies for materials with low bulk lifetimes. The simulation was carried out for a 300  $\mu\text{m}$  thick npp+ structure with an emitter sheet resistance of 80  $\Omega/\text{sq}$ , a front surface recombination velocity of  $S_F=10000 \text{ cm/s}$  and a rear surface recombination velocity of  $S_R=1000 \text{ cm/s}$  for 1  $\Omega\text{cm}$  material with  $S_R \propto N$  ( $N$ : dopant concentration) [8] for the different resistivities. A measured reflection of a SiN/MgF<sub>2</sub> DARC with a shadowing of about 4% is used. Further parameters are the shunt resistance with  $R_{\text{Sh}}=10000 \Omega/\text{cm}^2$ , the series resistance with  $R_S=0.5 \Omega/\text{cm}$  and  $j_{02}=2*10^{-8} \text{ A/cm}^2$ .

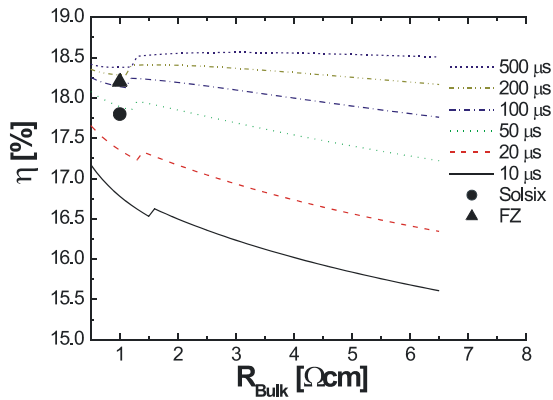


**Figure 4:** PC1D simulation for solar cells with different bulk resistivities and values reached for processed 2x2  $\text{cm}^2$  cells. The kink in the simulated curves seems to be an artefact of the PC1D program (incorrect mpp determination).

In Table I the highest values for each category are shown (EFG: 16 cells for each category, mc/FZ: 8 cells for each category). The efficiencies for the best EFG solar cells decrease strongly using resistivities below 2.2  $\Omega\text{cm}$  in contrast to the PC1D simulation. We believe that this is caused by increasing presence of poor quality areas for the higher doped EFG material.

$R_{\text{Bulk}}$	FF [%]	$j_{\text{sc}}$ [ $\text{mA}/\text{cm}^2$ ]	$V_{\text{oc}}$ [mV]	$\eta$ [%]
1.0 $\Omega\text{cm}$	78.9	32.9	609	15.8
1.6 $\Omega\text{cm}$	78.0	34.1	598	15.9
2.2 $\Omega\text{cm}$	79.0	35.2	603	16.8
2.6 $\Omega\text{cm}$	78.5	34.9	603	16.5
6.0 $\Omega\text{cm}$	77.6	35.7	599	16.6
mc (SiN)	79.1	35.8	630	17.8
mc (SiO/SiN)	79.2	35.9	635	18.0
FZ (SiN)	80.0	35.9	634	18.2
FZ (SiO/SiN)	79.5	36.1	639	18.3

**Table I:** IV-data of the best EFG solar cells from each resistivity class and solar cells from 1  $\Omega\text{cm}$  mc Solsix and FZ wafer reference material. In addition a SiO/SiN stack for an improved front surface passivation was tested for the references.

The 2.2  $\Omega\text{cm}$  class shows the highest IV values. The highest mean values are reached for the 2.6 and 6.0  $\Omega\text{cm}$  class (figure 5). The drop in efficiency at a certain

resistivity level is well known for EFG material. However, earlier studies showed that efficiency in EFG material decreases significantly for bulk resistivities below 3  $\Omega\text{cm}$  (with highest values about 4  $\Omega\text{cm}$ ) [6]. According to the results on state of the art EFG material this limitation moved towards 2  $\Omega\text{cm}$ . This shift is assumed to be the result of an improved EFG wafer manufacturing process within the last years. Due to a poor statistic of only 16 cells for each resistivity class it is hard to predict the optimal base doping. For reaching highest efficiency values on EFG material 2.2  $\Omega\text{cm}$  would be a good choice.

### 3.3 Hydrogenation via MIRHP

Former studies [3] showed that the fillfactor of the diced 2x2  $\text{cm}^2$  solar cells could be increased by about 1% absolute by an additional post processing hydrogenation using MIRHP. However,  $j_{\text{sc}}$  and  $V_{\text{oc}}$  seemed to remain constant by this additional hydrogenation. The increased fillfactor seems to be an effect of a slight edge passivation. Nearly all processed solar cells (figure 5) benefit from the MIRHP hydrogenation leading to increased fillfactor,  $j_{\text{sc}}$  and  $V_{\text{oc}}$ . This can not be explained with only an edge passivation and is assumed to be an effect of a bulk passivation (according to figures 2 and 3) and/or a surface passivation. For analyzing this effect IQE maps have been obtained for several solar cells before and after the additional hydrogenation using MIRHP. The IQE maps of two 1.6  $\Omega\text{cm}$  EFG solar cells before and after hydrogenation are illustrated in figure 6.

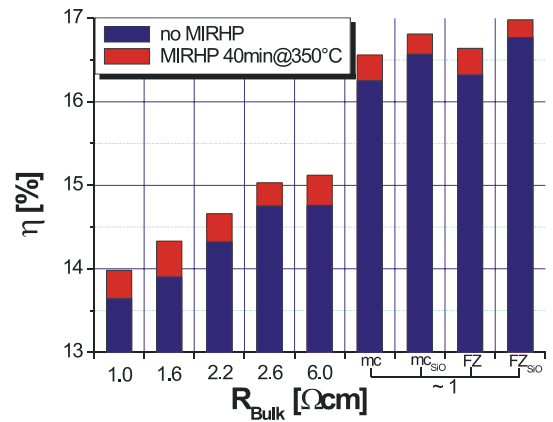


**Figure 5:** Efficiencies of EFG solar cells (without the second layer of the DARC) with different base resistivities before and after an additional hydrogenation by MIRHP. Mean values of 16 EFG cells and 8 mc/FZ cells for each class are given.

In figure 6 three area types can be distinguished. (1) are areas with very low lifetimes which can not be well hydrogenated leading to IQE values at 980 nm far below 0.4. These areas mainly limit cell efficiencies of the EFG solar cells presented in figure 5. (2) are areas of regular quality which can be improved by an additional hydrogenation by MIRHP and they are responsible for the major improvement of the IV data. (3) are areas with very high lifetimes often found in EFG material. These

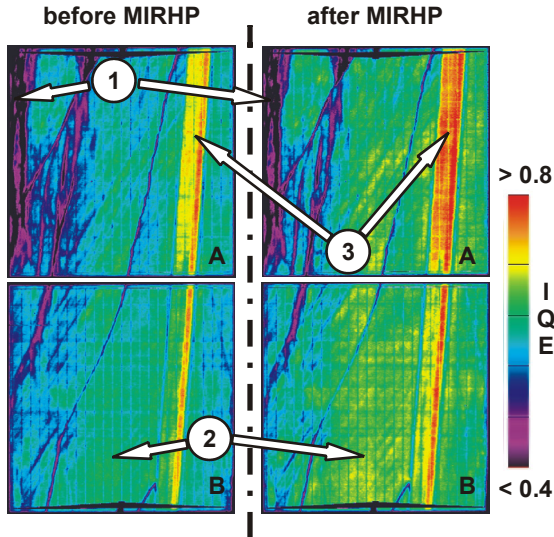


**Figure 6:** IQE Maps (980 nm) of two adjacent 1.6  $\Omega\text{cm}$   $2 \times 2 \text{ cm}^2$  EFG solar cells before (left) and after (right) an additional hydrogenation by MIRHP after cell processing.

areas get improved by MIRHP but the expected benefit on the IV values is small: on the one hand the increase in  $j_{sc}$  is small due to the area fraction and because an improvement of already good areas mainly affects the IQE only at long wavelengths, on the other hand  $V_{oc}$  is mainly determined and limited by the areas of type (1) and (2).

MIRHP	FF [%]	$j_{sc}$ [ $\text{mA}/\text{cm}^2$ ]	$V_{oc}$ [mV]	$\eta$ [%]
before (A)	77.7	30.0	579	13.5
after (A)	78.1	30.5	582	13.9
before (B)	78.1	30.6	588	14.0
after (B)	78.7	31.0	592	14.6

**Table II:** IV data of the two EFG solar cells A and B shown in figure 6 before and after an additional hydrogenation by MIRHP (without the second layer of the DARC).

Table II shows in detail the benefit of the additional hydrogenation by MIRHP on the specific IV data. The main improvement can be found in the  $j_{sc}$  values due to a better spectral response at long wavelengths for a large part of the cell area visible in the IQE maps in figure 6. The difference between cell A and B is that in cell B extended areas of type (1) can not be found. Therefore  $V_{oc}$  and  $j_{sc}$  are considerably higher for cell B leading to a 0.5% higher efficiency before and 0.7% higher efficiency after an additional MIRHP hydrogenation. So the cell with less very poor areas (1) improves more after the MIRHP hydrogenation. It would be of interest if EFG material with SiN fired by a rapid thermal anneal is affected in the same way by a subsequent hydrogenation using MIRHP.

In [3] an efficiency of 17.2% on 3  $\Omega\text{cm}$  EFG material was reported using a refractive index of 2.0 for the SiN layer leading to higher reflectivities as obtained for the solar cells presented in this contribution. We therefore think that EFG material of similar quality as used in [3] will lead to efficiencies close to 18% using the optimized cell process presented here, as could be demonstrated by the references, provided bulk lifetimes are high enough.

#### 4 SUMMARY

Gettering followed by hydrogenation has a strong benefit on the IV data for solar cells processed on EFG material. Several studies showed that hydrogenation by firing a hydrogen rich SiN layer is the best choice for hydrogenation of EFG material. For conventional firing in a belt furnace it was shown that an additional hydrogenation by MIRHP improves both the minority carrier lifetimes and the IV data of EFG solar cells. Hydrogen can diffuse through a rear side aluminum layer [9] and the SiN layer at the front side is assumed to be a diffusion barrier for the hydrogen leading to only a one-sided indiffusion of hydrogen from the rear. Therefore the chosen temperatures and durations used for the MIRHP hydrogenation of the readily processed solar cells could be too low for an even more sufficient second bulk hydrogenation.

Below a bulk resistivity of 2.2  $\Omega\text{cm}$  IV values of EFG solar cells drop significantly. Earlier studies showed that the quality of EFG material decreases strongly with a bulk resistivity below 3  $\Omega\text{cm}$ . The shift of this value to currently 2.2-2.6  $\Omega\text{cm}$  seems to be the result of an improved wafer fabrication technology within the last years.

#### 5 ACKNOWLEDGEMENTS

The underlying project of parts of this report was supported with funding of the German BMU under contract number 0329846J and by the EC (SES6-CT-2003-502583). The content of this publication is the responsibility of the authors. We thank Stephan Eisert for assistance during solar cell processing.

#### 6 LITERATURE

- [1] A.Rohatgi, D.S.Kim, V.Yelundur, K.Nakayashiki, A.Upadhyaya, M.Hilali, V.Meemongkolkiat, Technical Digest of the 14<sup>th</sup> PVSEC, Bangkok 2004, p. 635
- [2] P.Geiger, G.Kragler, G.Hahn, P.Fath, E.Bucher, Sol. En. Mat. & Solar Cells 85, 2005, p. 559
- [3] M.Kaes, G.Hahn, A.Metz, Proc. 31<sup>st</sup> IEEE PVSC, Lake Buena Vista 2005, in press
- [4] B.Damiani, K.Nakayashiki, D.S.Kim, V.Yelundur, S.Ostapenko, I.Tarasov, A.Rohatgi, Proc. 3<sup>rd</sup> WCPEC Osaka 2003, p. 927
- [5] G.Hahn, P.Geiger, Progr. Photovolt.: Res. Appl. 11, 2003, p. 347
- [6] B.R.Bathey, J.P.Kalejs, M.D.Rosenblum, M.J.Kardauskas, R.M.Giancola, J.Cao, Proc. 28<sup>th</sup> IEEE PVSC, Anchorage 2000, p. 194
- [7] D.A.Clugston, P.A.Basore, Proc. 26<sup>th</sup> IEEE PVSC, New York 1997, p. 207
- [8] M.P.Godlewski, C.R.Baraona, H.W.Brandhorst, Proc. 10<sup>th</sup> IEEE PVSC, Palo Alto 1973, p. 40
- [9] G.Hahn, D.Sontag, S.Seren, A.Schönecker, A.R.Burgers, R.Ginige, K.Cherkaoui, D.Karg, H.Charifi, Proc. 19<sup>th</sup> EC PVSEC, Paris 2004, p. 427